# Chapter 5
# Lead Theory of Differential Leads and Synthesis of the Standard 12-Lead ECG

**Abstract** In this chapter, the lead theory of differential leads is presented. A differential lead is an ECG lead obtained from two closely positioned electrodes on the body surface. It can be measured with an ECG body sensor. The theoretical background is needed to gain a formal and intuitive understanding of what is measured with differential leads, as well as to elaborate how the standard 12-lead ECG can be synthesized from three differential leads. The 12-lead ECG synthesis is based on the dipole volume source model. After introducing the dipole model, the Burger's equation is derived and the concept of lead vector defined. We describe how to derive lead vectors from known heart vector and, vice versa, how to obtain the heart vector from known lead vectors. Then, the concepts of image surface and lead field are introduced, followed with a description of the lead field of a differential lead. Next, the theory and methods for ECG leads synthesis from differential leads is presented. The chapter concludes with a discussion on the evaluation and personalization of the synthesis.

## 5.1 Preconditions

Depending on the purpose, different assumptions will be made throughout this chapter regarding the characteristics of the volume source and the volume conductor. Common assumptions of the lead theory are that *a human body is a quasi-static and linear physical system*.

Cardiac electrical sources are a consequence of the electrical activity of the myocardium cell membranes, i.e., of ion flows through the membranes. Since these activities vary with time (different cells and different numbers of cells are depolarized or repolarized), the resulting electrical potential field established in the volume conductor is time-varying. The quasi-static assumption states that all the fields: those in the volume source, i.e. in the heart, and those in the volume conductor, i.e. in the body, are synchronous, as if the sources were static. In other words, at any time instant, the electrical field throughout the body, or the resulting potential field at the body surface, will be a consequence of a stationary source at the same instant. A consequence of the quasi-static conditions is that from the distribution of sources at



R. Trobec et al., *Body Sensors and Electrocardiography*, SpringerBriefs in Applied Sciences and Technology, DOI 10.1007/978-3-319-59340-1_5

a given time instant, the corresponding extra-cardiac field can be determined without any regard to the source distribution in the past.

For the *quasi-static* conditions to be met, the following should be satisfied [3]:

1. negligible propagation effect, i.e., negligible time required for the propagation of changes in the source to any field point,
2. negligible capacitive effect,
3. negligible inductive effect.

By using the electrical properties of biological materials previously reported by Rush et al. [1] and Schwan and Kay [2], Plonsey and Heppner [3] showed that the above conditions are met for frequencies up to 1 kHz and for distances up to 1 m.

For an intuitive justification and understanding of the quasi-static nature of the bioelectrical phenomena, it is helpful to consider the rate of change of the involved fields, which is not fast enough to prevent the consequential potential field on the body surface from being observed at the moment when the change of the source field occurs.

The *linearity* of the system means that whenever a source is increased by a factor, the resulting potential field will be increased by the same factor. The linearity also means that a linear combination of sources produces a linear combination of responses that would have been caused by each source individually. This property of linear systems is also called *the principle of superposition* or the superposition property.

In summary, the resulting potential field and currents through the volume conductor at any time instant depend only on the sources at that instant and obey the principle of superposition.

## 5.2 Dipole as a Volume Source Model

An important task in electrocardiography is to solve the inverse problem, i.e., to determine or estimate the electrical sources in the heart that resulted in a measured potential distribution on the body surface (or some other describable surface) at each instant of time. It is, however, obvious that for any three-dimensional potential distribution, there is an infinite number of electrical cardiac sources that can induce it [4–6]. This is because one can always add sources that generate no field or a field below the noise level.

After we have established that there is no unique mapping between body surface potentials and electrical sources in the heart, it is evident that the inverse problem can be solved only if a model of the volume source is assumed. To solve the inverse problem then means to determine the value of the parameters describing the assumed model. Please note that the solution of the inverse problem is always just a model, and consequently does not exist in reality.

There are different possible models for the volume source, e.g. dipole, quadrupole, octapole, and so on, and finally multipole. A model that generates the same potentials

on the body surface as the actual primary source is called *equivalent source* or *equivalent generator*. The multipole is an example of such a model [6]. We will, however, concentrate on the dipole model, since it is the central model used in ECG synthesis theory. Furthermore, it will be shown that cardiac electrical activity on the body surface can be predominately explained by the dipole volume source model.

Geselowitz has shown in [6] that the heart dipole can be expressed in terms of impressed currents as:

$$\vec{p_H} = \int_{V_H} \vec{J}^i dV - \sum_j \int_{S_j} (\sigma' - \sigma'')\phi d\vec{S}_j, \tag{5.1}$$

where $V_H$ is the heart volume, $\vec{J}^i$ is the impressed current density associated with the active behavior of the cell membranes, $d\vec{S}_j$ is a differential element of the surface $S_j$ that separates regions of conductivity $\sigma'$ and $\sigma''$, and $\phi$ is the potential at $d\vec{S}_j$. Note that $d\vec{S}_j$ is a vector surface element that is by convention directed from the $\sigma'$ region towards the $\sigma''$ region. The equation provides an arbitrary number of surfaces $j$ that separate regions of different conductivities. The major discontinuities in conductivity are inner and outer surfaces of the heart, i.e., the surface between the myocardium and the intracavitary blood mass, and the surface between the myocardium and the lungs.

For a homogeneous conductor, $\sigma' = \sigma'' = \sigma$ applies, so that the previous Eq. 5.1 reduces to:

$$\vec{p_H} = \int_{V_H} \vec{J}^i dV, \tag{5.2}$$

which indicates that $\vec{J}^i$ is a dipole moment per unit volume (i.e., the dipole density) and $\vec{J}^i dV$ is a single dipole source component of the heart dipole $\vec{p_H}$. Therefore, the heart vector can be considered as a sum of all the elementary dipole contributions throughout the entire volume of the heart $V_H$. Note that $\vec{J}^i$ changes in time, because the heart electrical activity is different in different time moments. Consequently, the vector $\vec{p_H}$ changes its magnitude, direction and location through time. Note that the terms "heart dipole" and "heart vector" are used as synonyms. We denote the exact heart vector $\vec{p_H}$ with subscript $H$ to distinguish it from all the other fictitious dipoles used to model a heart, which are also commonly called heart vectors.

The heart dipole, as expressed by Eq. 5.1, is only the first term of the possible multipole expansion that provides a complete description of the equivalent generator [6]. An obvious, but important consequence is that the heart dipole does not produce the same potential distribution on the body surface as the real heart source or an equivalent generator. Still, as we are going to see in Sect. 5.7.1, there is a lot of evidence that the heart is predominately a dipolar source. Even though the recording sites can be close to the heart, depending on the employed lead system, additional justification for considering the heart as a dipole comes from the fact that any complex source with a zero net current can be approximated by a dipole, with an improvement in approximation as the observation distance becomes greater than the largest

dimension of the source [7]. The condition of net current, i.e., the algebraic sum of currents being equal to zero, is satisfied by the heart since no net charge is generated at any instant.

The heart dipole $\vec{p_H}$ has a location that is time-dependent. As the observation distance from the heart increases, the dislocation of $\vec{p_H}$ from the heart centroid becomes more and more negligible. Therefore, the vector $\vec{p_H}$ is sometimes assumed to be at the center of the heart region, although its position is time-dependent. The source model which assumes a dipole with a fixed location and variable orientation and magnitude is called *fixed dipole model*. On the other hand, the source model which assumes not only varying orientation and magnitude, but also varying location for a single dipole, is called *moving dipole model*. Depending on the purpose, the location of the heart dipole can be relevant or irrelevant. It is important to note that to uniquely describe a fixed dipole, its three Cartesian coordinates (or in spherical coordinates: magnitude and two direction angles) are necessary. For describing a moving dipole, however, six independent variables are necessary: three for describing the dipole vector and three for describing the dislocation vector.

## 5.3 Lead Vector

Einthoven's classical lead theory [8, 9] is based on the assumption that the human body is a part of a spherical or an infinitive homogeneous conductor, in which the heart electrical sources are represented by a single, two-dimensional time-varying dipole that has a fixed location in the frontal plane of the human body, at the center of the homogeneous sphere. Burger and van Milaan developed a more precise lead theory, referred to as the volume-conductor theory [10, 11], by assuming that the human body is a three-dimensional, bounded, irregularly shaped and inhomogeneous volume conductor. Their lead theory also relies on the fixed dipole hypothesis. According to it, the potentials anywhere on the body surface can be derived by projecting the heart dipole on directions in three dimensional space called lead vectors.

The lead vector is a concept that provides ECG leads with a formal spatial interpretation. It is a time-invariant vector in space describing the direction in which a certain lead monitors the cardiac electrical activity. The length of the lead vector determines the lead measurement sensitivity. Figure 5.1 shows the Einthoven triangle of limb lead vectors obtained under Einthoven's assumptions.

The Burger's equation formally relates the voltage on a given lead to its lead vector:

$$L = \vec{L} \cdot \vec{p}, \tag{5.3}$$

where $\vec{p}$ is a dipole describing the cardiac electrical activity, not necessarily equal to $\vec{p_H}$. For instance, $\vec{p}$ can be an artificial dipole placed in a volume conductor model for experimental purposes.

As an example of the Burger's equation application, consider the case where two points determining a bipolar lead are on the left and the right arms (Fig. 5.1).

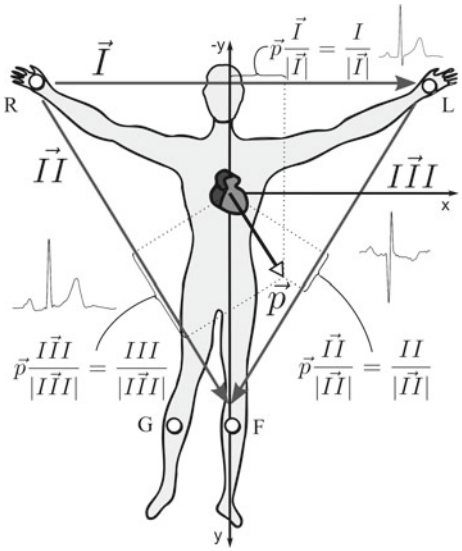


**Fig. 5.1** Einthoven triangle. All the lead vectors lie in the frontal plane of the human body, defined by the x-y coordinate system vectors. The projections of the heart vector $\vec{p_H}$ on the sides of the triangle are equal to the scalar product of the heart vector and the normalized lead vectors (Burger's equation)

According to the Burger's equation 5.3, the measured voltage of the bipolar lead is: $I = \vec{I} \cdot \vec{p}$.

The Burger's equation is in fact the definition of the lead vector—the vector that, when multiplied by the dipole representing the heart, provides the measured lead voltage. The Burger's equation is also a statement that such a vector exists for every choice of the vector $\vec{p}$. The question remains how to obtain the lead vector for a specific lead. From the Burger's equation, it is obvious that to calculate $\vec{L}$, one needs to know the voltage measured on a lead and the vector $\vec{p}$. Normally, one would employ a model of the volume conductor inside which a dipole is energized and measure potentials on the model's surface. More details on the procedure for obtaining lead vectors are provided in Sect. 5.3.2.

For the scalar product $\vec{L} \cdot \vec{p}$ to be evaluated by $L = |\vec{L}| \cdot |\vec{p}| \cdot \cos(\theta)$, where $\theta$ is the angle between the vectors, the location of $\vec{p}$ and $\vec{L}$ relative to each other is irrelevant. Hence, the vectors $\vec{L}$ and $\vec{p}$ can be placed at the origin of an arbitrary coordinate system. The system is normally chosen to have origin at the position of the negative pole of $\vec{p}$ (see Fig. 5.2). The rationale for this choice comes from the fact that the orientation and length of each lead vectors $\vec{L}$ depends on the locations of the corresponding vector $\vec{p}$ (will be explained in Sect. 5.5). It is, therefore, convenient to give each vector $\vec{p}$ and the corresponding vector $\vec{L}$ a common starting point.

The Burger's equation was derived under the assumption that the inhomogeneous and irregularly shaped human body is a linear physical system (Sect. 5.1). Besides the location of the vector $\vec{p}$, the vector $\vec{L}$ also reflects the inhomogeneities and the shape of the volume conductor, when deriving the lead voltage from a known $\vec{p}$. More details on this are provided in Sect. 5.5.

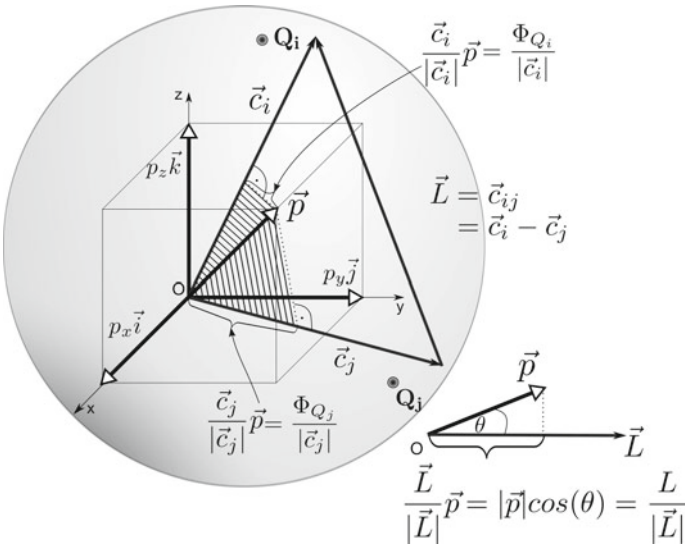


**Fig. 5.2** Heart vector projections on axes and leads. $\vec{c}_i$ and $\vec{c}_j$ are the unipolar lead vectors for the points $Q_i$ and $Q_j$, respectively, whereas $\vec{L}$ is the bipolar lead vector. The projection of the heart vector on a lead vector, multiplied by the length of the lead vector, is the lead voltage. The medium (volume source and volume conductor) is conductive, linear, and inhomogeneous

### *5.3.1 The Burger's Equation*

A dipole is a pair of a current source and a current sink of the same current strength $I_d$ and separated by a small displacement $d$. The mathematical definition of a dipole requires $d \to 0$, $I_d \to \infty$, with $p = I_d \cdot d$ remaining finite. The quantity $p$ is the moment or magnitude of the dipole. The dipole is a vector $\vec{p}$ with magnitude $p$ and direction from the negative source (sink) towards the positive source [12].

It is worth noting that "perfect" mathematical dipoles, i.e., dipoles with $d \to 0$, do not exist in electrophysiology. The "real" physical dipoles, like those formed on cell membranes, have a displacement greater than zero (e.g. membrane thicknesses). Still, mathematical dipoles are often used as an approximation for physical dipoles, for practical reasons, because the mathematical dipoles are described with concise formulas. The approximation of physical dipoles as mathematical dipoles holds for $d/r < 0.1$, where $r$ is the displacement from the dipole, i.e., if the observation distance is at least ten times larger than the displacement of the monopoles forming the dipole [13].

Let us assume a three-dimensional coordinate system $(\vec{i}, \vec{j}, \vec{k})$ with a reference potential located at its origin. Let $\phi_Q^{\vec{i}}$ be the potential at an arbitrary point Q caused by the unit dipole $\vec{i}$. By using the linearity assumption, the potential $\phi_Q^{p_x\vec{i}}$ corresponding to the dipole $p_x\vec{i}$ of an arbitrary magnitude $p_x$ is:

$$\phi_Q^{p_x\vec{i}} = \phi_Q^{\vec{i}} \cdot p_x. \tag{5.4}$$

An analogous expression holds for the dipoles in the $\vec{j}$ and $\vec{k}$ directions. The linearity assumption ensures the maintenance of the principle of superposition, which states that an electrical field arising from several sources is the sum of the fields that would be present if each source acted separately. The dipole in three orthogonal components is:

$$\vec{p} = p_x\vec{i} + p_y\vec{j} + p_z\vec{k}. \tag{5.5}$$

Using the principle of superposition, the potential at the point $Q$, caused by the dipole $\vec{p}$ at the origin of the coordinate system, is:

$$\phi_Q^{\vec{p}} = \phi_Q^{\vec{i}} p_x + \phi_Q^{\vec{j}} p_y + \phi_Q^{\vec{z}} p_z. \tag{5.6}$$

If components $\phi_Q^{\vec{i}}, \phi_Q^{\vec{j}}$ and $\phi_Q^{\vec{k}}$ are interpreted as the components of a vector $\vec{c}$, Eq. 5.6 can be written as:

$$\phi_Q^{\vec{p}} = \vec{c} \cdot \vec{p}. \tag{5.7}$$

The vector $\vec{c} = (\phi_Q^{\vec{i}}, \phi_Q^{\vec{j}}, \phi_Q^{\vec{k}})$ is called *lead vector of a unipolar lead*. In this case, the lead is determined by the potential at the point $Q$ and the zero potential at the origin of the coordinate system, but in general, the zero reference potential can be any local or remote reference point.

A bipolar lead whose electrodes are at points $Q_i$ and $Q_j$ measures the potential difference $L$ between the two points:

$$V_{Q_1Q_2} = L = \phi_{Q_i}^{\vec{p}} - \phi_{Q_j}^{\vec{p}}. \tag{5.8}$$

In the following, we will use $L$ instead of $V_{Q_1Q_2}$ to designate a lead voltage in situations not requiring reference to the names of the points $Q_1$ and $Q_2$ that determine the lead. By substituting $\phi_{Q_i}^{\vec{p}}$ and $\phi_{Q_j}^{\vec{p}}$ according to Eq. 5.7, in Eq. 5.8, we get the Burger's equation:

$$L = \vec{c}_i\,\vec{p} - \vec{c}_j\,\vec{p} = \vec{c_{ij}} \cdot \vec{p} = \vec{L} \cdot \vec{p} = |\vec{L}| \cdot |\vec{p}| \cdot \cos(\theta), \tag{5.9}$$

where $\vec{c_i}$ and $\vec{c_j}$ are unipolar lead vectors for the points $Q_i$ and $Q_j$, $\vec{L} = \vec{c_{ij}} = \vec{c_i} - \vec{c_j}$ is *the bipolar lead vector*, and $\theta$ is the angle between $\vec{L}$ and $\vec{p}$.

From Eq. 5.9, it follows that for a normalized lead vector, i.e. for $|\vec{L}| = 1$, the lead voltage L is $|\vec{p}| \cdot \cos(\theta)$—the projection of the heart vector on the lead vector. The same holds for the unipolar lead vector from Eq. 5.7. This is why a lead vector can be interpreted as a spatial direction in which the cardiac electrical activity is monitored. It follows from Eq. 5.9 that the lead voltage $L$ is obtained by multiplying the heart vector's projection with the length of the lead vector $|\vec{L}|$. Consequently, a longer $\vec{L}$ implies a higher measured voltage. For this reason, the length of a lead vector $|\vec{L}|$ is also called *the lead sensitivity*. Alternatively, a lead vector can be thought of as a

sensitivity vector with the length representing the magnitude of the lead sensitivity, whereas the direction is the direction of the lead sensitivity.

The voltage on the left side of the Burger's equation is the only directly measurable entity in living subjects. Therefore, to have a control over $\vec{p}$, a model is usually used. Then, if we know the heart vector $\vec{p}$, the Burger's equation can be applied to determine the lead vector. The Burger's equation is used also in the opposite direction: to determine $\vec{p}$ from known lead vectors. In the continuation, we will show that three lead vectors are needed for this purpose.

### 5.3.2 Deriving the Lead Vectors from a Known Heart Vector

Equation 5.6 can be used to experimentally find a lead vector for an arbitrary point $Q$ on a body surface by using a mathematical or a physical torso model. The lead vector is found by energizing unit dipoles in the model's heart region along the $x$, $y$, and $z$ axes in sequence, and measuring the potential at the point $Q$ for each dipole. For example, if the unit dipole is oriented in the $x$ direction, then $p_y = p_z = 0$. From Eq. 5.6, it follows that $\phi_Q^{\vec{i}} = \phi_Q^{\vec{p}}$. Since $\phi_Q^{\vec{p}}$ is the measured potential, the first element of the vector $\vec{c}$ is determined.

It is important to note that the lead vectors are not derived (and not even defined—see Eq. 5.3) by using real heart electrical sources (like, for instance, an equivalent dipole defined by Eq. 5.2) and a real volume conductor, but by experimentally placing a dipole on a fixed location in a model of a volume conductor. The more the fixed dipole is a realistic model of the source (see Sect. 5.7.1), and the more the model of the volume conductor is realistic and appropriate for each person, the more the calculated lead vectors are reliable representations of the corresponding leads' observational directions and sensitivities. Since the use of the models is in practice the only way for determining the lead vectors, it can be said that a lead vector is a vector in space, which when multiplied by a dipole source, results in a corresponding measured potential on the surface of the employed volume conductor model.

Even though lead vectors for individual $\vec{p_H}$ defined by Eq. 5.1 cannot be precisely determined in practice, they do exist in theory, since the Burger's equation states that there is always a vector $\vec{L}$ on which one vector $\vec{p}$ can be projected to produce the measured voltage. Even if we consider the $\vec{p_H}$ location as time-dependent, then for each moment in time, there is still a $\vec{L}$ that when multiplied by $\vec{p_H}$ would produce the measured voltage. Nevertheless, $\vec{L}$ is by definition time-invariant and defined for a fixed location dipole.

### 5.3.3 Deriving the Heart Vector from Known Lead Vectors

A dipole $\vec{p}$ describing a heart, as any other vector in space, at each instant in time has three components in Cartesian coordinates (see Eq. 5.5). To calculate the three

components, one needs a system of three equations with the three components as the only unknowns. We write three Burger's equations for the three leads:

$$L(i) = \vec{L}(i) \cdot \vec{p}, \; i = 1, 2, 3, \tag{5.10}$$

where $i$ indexes the leads. If the three lead vectors $\vec{L}(i)$ are known a priory and if we can measure voltages on the three leads $L(i)$, then we can solve the system of Eq. 5.10 for the three components of the vector $\vec{p}$. Note that if the lead voltages are measured on a real person, but the lead vectors were previously determined by using a model (as described in Sect. 5.3.2), this procedure, in the absence of noise, results in $\vec{p}$ that, if inserted in the same model, would produce voltages equal to the voltages measured on the person. Consequently, the obtained heart vector is not equal to the heart vector defined by Eq. 5.1 and is only an estimate of it. Additionally, the vector $\vec{p_H}$ defined by Eq. 5.1 is a moving dipole, whereas the obtained vector $\vec{p}$ is fixed. In conclusion, any three independent leads suffice for an accurate representation of a fixed-location dipole, which is an estimate of the heart vector.

## 5.4 Image Surface

According to the procedure described in Sect. 5.3.3, the cardiac electrical activity can be described by measuring the potentials on leads with known lead vectors. It is therefore desirable to know the unipolar lead vectors for any point on a body surface.

The concept of determining lead vectors described in Sect. 5.3.2 can be applied at an arbitrary number of points on a model surface. The tips of the acquired unipolar lead vectors determine the surface known as *the image surface* or image space. Since it consists of lead vectors, an image surface can be interpreted as an alternative, imaginary torso, in which lines connecting two points represent the true monitored spatial directions of the cardiac electrical activity. The deviation of each lead vector's direction from the direction defined by the line connecting the lead's electrode positions on the body surface can be regarded as a measure of the electrical distortion of the dipole behavior as seen on the body surface [14].

The concept of image surface was introduced by Burger and van Milaan [15], but its first experimental determination was performed by Frank [16]. As a collection of lead vectors, the image surface depends on the location of the dipole and the characteristics of the volume conductor. Consequently, image surfaces are different for each person. The image surfaces are practically obtained by using physical models which are designed to be representative for all people or for a particular population.

Among all existing image surfaces, the Frank image surface, published in [16], is the one most often used in the subsequent research. Frank constructed a tank model having a thorax form, oriented it upside-down, and filled it with a salt solution. A dipole was fixed in the center of the model region, which Frank assumed to be "occupied in life by the ventricular mass during very deep inspiration". The frontal-view-triangle part of the Frank image surface can be seen to depart significantly from the equilateral Einthoven triangle, i.e., the limb lead vectors in the Frank image space

are different from the Einthoven triangle lead vectors. This is because the Frank's model is not spherical, whereas the Einthoven's model is spherical, even though both models are homogeneous. For a complete specification of the Frank image surface, the reader is referred to [16].

Frank also stated that the influence of the dipole location on the lead vectors is more pronounced than the influence of the torso's shape and the inhomogeneities introduced into the model [4]. More recent image surface studies were made on computer models. Computer models make it easier to include more detailed inhomogeneities, such as intracavitary blood masses and muscle layers, as well as to investigate the influence of the dipole location on the image surface [17]. The research on computer models did not invalidate Frank's observations.

## 5.5 Lead Field

A lead field is a vector field consisted of lead vectors obtained for different locations of a dipole, by keeping the lead measurement points fixed. Each lead vector is placed at the position of the dipole for which it is derived. The lead field approach is opposite to the image surface approach, in which the dipole position is kept constant, while the measurement point positions are varied. We use the notation $\vec{L}(x, y, y)$ to designate a lead vector field, and $\vec{L}$ to designate a single lead vector. Given the vector field $\vec{L}(x, y, y)$, we can extend the Burger's equation 5.3 and write:

$$L = \vec{L}(x, y, y) \cdot \vec{p}(x, y, y). \tag{5.11}$$

This equations states that the measured voltage for a lead is a product of a dipole $\vec{p}$ describing the heart and the element of the lead's vector field $\vec{L}(x, y, y)$ at the same location as $\vec{p}$.

To determine the lead field for a pair of positions on the body surface, one needs to calculate lead vectors for every dipole position in a model, using the procedure described in Sect. 5.3.2. In practice, that is possible only for a finite number of dipole positions. Fortunately, there is another way of describing a lead field. The alternative approach is based on *the electromagnetic reciprocity theorem*, which states roughly the following: The relationship between a current and the resulting electric field is unchanged if one interchanges the points where the current is placed and where the field is measured. In other words, if the current source and voltmeter positions are swapped, the voltmeter reading will not be altered.

Let there be an approximate dipole formed by a point source $I_d$ and a point sink $-I_d$ at a very small distance $d$ in an arbitrarily shaped volume conductor. This dipole can be a heart vector $\vec{p_H}$:

$$\vec{p_H} = I_d \vec{d}. \tag{5.12}$$

Let $\phi'$ be the potential field of $\vec{p_H}$. Then, the voltage between the points $Q_1$ and $Q_2$ is (panel A in Fig. 5.3):

$$V_{Q_1 Q_2} = \phi'(\vec{r_{Q_1}}) - \phi'(\vec{r_{Q_2}}). \tag{5.13}$$

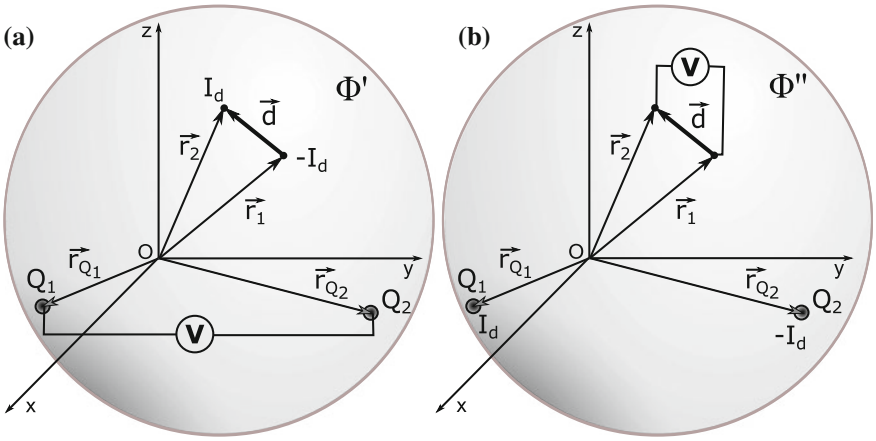


**Fig. 5.3** The application of the reciprocity theorem: before and after swapping the positions of the source ($I_d$) and the voltmeter (V), as shown on the panels (**a**) and (**b**), the voltmeter will measure the same voltage

By applying the Burger's equation 5.3, we can also write:

$$V_{Q_1Q_2} = L = \vec{p_H} \cdot \vec{L}_{Q_1Q_2}, \tag{5.14}$$

where $\vec{L}_{Q_1Q_2}$ is the lead vector for the measured voltage $V_{Q_1Q_2} = L$.

If we swap the positions of the current source and the voltmeter (panel B in Fig. 5.3), the reciprocity theorem states that:

$$V_{Q_1Q_2} = \phi''(\vec{r_2}) - \phi''(\vec{r_1}), \tag{5.15}$$

where $\phi''$ is the potential field of the point source $I_d$ and the point sink $-I_d$ placed at $Q_1$ and $Q_2$, respectively.

Since $d$ is assumed to be small, to obtain $\phi''(\vec{r_2})$, we can write the Taylor expansion for $\phi''$ at $\vec{r_1}$ by including only the linear term:

$$\phi''(\vec{r_2}) = \phi''(\vec{r_1}) + \frac{\partial \phi''}{\partial d}\bigg|_{\vec{r_1}} \cdot d. \tag{5.16}$$

Since the directional derivative (the second element on the right side of Eq. 5.16) is the same as the gradient multiplied by the unit vector in that direction, it follows:

$$\phi''(\vec{r_2}) = \phi''(\vec{r_1}) + \nabla\phi'' \cdot d \cdot \vec{a}_d = \phi''(\vec{r_1}) + \nabla\phi'' \cdot \vec{d}, \tag{5.17}$$

where $\vec{a}_d$ is the unit vector in the direction $\vec{d}$. By inserting Eq. 5.17 in Eq. 5.15, we obtain:

$$V_{Q_1Q_2} = \nabla\phi'' \cdot \vec{d}. \tag{5.18}$$

Since the potential field caused by a dipole ($\phi_D$) is proportional to $I_d$ [13]:

$$\phi_D = \frac{I_d}{4\pi\sigma}\nabla(\frac{1}{r})\vec{d}, \tag{5.19}$$

it follows that a unit current $I_0$ used instead of $I_d$ would produce the potential field $\phi_0''$ such that $\frac{\phi_0''}{\phi''} = \frac{I_0}{I_d}$. So, the potential field of a general dipole, with respect to a field of a dipole with unit current, is $\phi'' = \phi_0'' \cdot \frac{I_d}{I_0}$. If we apply the latter to Eq. 5.18, we get:

$$V_{Q_1Q_2} = \frac{\nabla\phi_0''}{I_0} \cdot I_d\vec{d} = \frac{\nabla\phi_0''}{I_0} \cdot \vec{p_H}, \tag{5.20}$$

where $I_d\vec{d} = \vec{p_H}$ as stated in Eq. 5.12. Note that $\frac{\nabla\phi_0''}{I_0} \cdot \vec{p_H}$ is a scalar product of a single vector and a vector field, or in other words, the product of $\vec{p_H}$ and the corresponding vector at the same position in $\nabla\phi_0''$. By comparing Eqs. 5.20 and 5.14, it is obvious that:

$$\vec{L}_{Q_1Q_2}(x, y, z) = \frac{\nabla\phi_0''}{I_0}, \tag{5.21}$$

where $\vec{L}_{Q_1Q_2}(x, y, z)$ is the lead field for the lead defined by the points $Q_1$ and $Q_2$. $\vec{L}_{Q_1Q_2}(x, y, z)$ is used to express that it refers to a vector field, compared to $\vec{L}_{Q_1Q_2}$, which is a single vector.

Equation 5.21 states that a lead field is equal to the gradient of the potential field caused by a pair of a unit current source and a sink placed at the lead's electrodes positions. For an intuitive representation of a lead field, it is helpful to take into account that the current density in the volume conductor is directly proportional to the gradient of the potential $\vec{J}_0^L = -\sigma\nabla\phi_0''$. If we apply this fact to Eq. 5.21, we get:

$$\vec{L}_{Q_1Q_2}(x, y, z) = \frac{\nabla\phi_0''}{I_0} = \frac{-\vec{J}_0^L}{I_0\sigma}, \tag{5.22}$$

where $\vec{J}_0^L = \vec{J}_0^L(x, y, z)$ denotes the current density due to unit reciprocal current. Hence, the lead field structure for the lead defined by two electrodes is equivalent to the structure of the current density between the same two electrodes, but respecting that the current and the potential gradient have opposite directions (see Fig. 5.4).

If we consider the heart vector to be the sum of all the elementary dipole contributions (Eq. 5.2), we may apply the superposition principle on Eq. 5.20, to obtain:

$$V_{Q_1Q_2} = L = \int \frac{\nabla\phi_0''}{I_0} \cdot \vec{J}^i dV = \frac{1}{I_0}\int \left(\frac{-\vec{J}_0^L}{\sigma}\right) \cdot \vec{J}^i dV, \tag{5.23}$$

where $\sigma$ is the conductivity distribution through the heart volume, which is in general a function of position and time: $\sigma = \sigma(x, y, z, t)$, and $\vec{J}^i$ is the volume

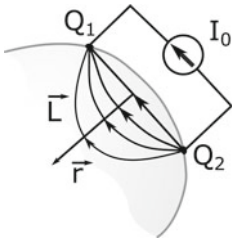


**Fig. 5.4** The lead field of a differential lead. The *lines* with *arrows* within the volume conductor (*gray circle*) represent the lead field $\vec{L}$. The lead field is proportional to the current flow field arising from a unit current introduced at $Q_1$ and removed at $Q_2$, and has the opposite direction. The bowing of the field increases with $r$, whereas the field magnitude (i.e., the current strength) decreases with $r^3$

source impressed current vector field, which also depends on position and time: $\vec{J}^i = \vec{J}^i(x, y, z, t)$. If $\sigma$ is constant, we can move $\frac{1}{\sigma}$ out of the integral and obtain:

$$V_{Q_1Q_2} = \frac{-1}{I_0\sigma} \int \vec{J}_0^L \cdot \vec{J}^i dV. \tag{5.24}$$

Equations 5.23 and 5.24 show that each element $dV$ of the volume source contributes to the lead voltage with a component equal to the scalar product of the lead field current density at $dV$ and the volume source impressed current element, divided by the conductivity at the same spatial element $dV$. In other words, the lead voltage is a weighted sum of contributing sources with weights $\nabla\phi_0'' = (\frac{-\vec{J}_0^L}{\sigma})$. This justifies the interpretation of the lead field as *the lead sensitivity distribution*, as its role in obtaining the lead voltage is to weight each source element $\vec{J}^i$. A larger magnitude of $\vec{J}_0^L$ at $dV$ and a smaller angle between $\vec{J}^i$ and $\vec{J}_0^L$ at $dV$ result in a larger contribution of $\vec{J}^i$ at $dV$ to the measured voltage.

Recall that we described (Sect. 5.3.1) the lead vector as the sensitivity vector for one location of a dipole. The lead field is an extension of the lead vector concept for all locations of the dipole. Consequently, one lead vector, obtained for one location of the dipole, is an element of the lead field obtained by using the same model (recall that the lead vectors are always derived by using a model—Sect. 5.3.2). Multiplying $\vec{p}_H$ by its lead vector (Eq. 5.20), and multiplying each $\vec{J}^i dV$ by its lead vector and then summing the products for all $dV$s (Eq. 5.23), is equivalent in terms of producing the same voltage $V_{Q_1Q_2}$ (Eqs. 5.20 and 5.23 have the same $V_{Q_1Q_2}$ on the left). According to Eq. 5.20, $V_{Q_1Q_2}$ is caused by $\vec{p}_H$. The real distribution of sources $\vec{J}^i$ produces a voltage different from $V_{Q_1Q_2}$, because $\vec{p}_H$ is not an equivalent generator (as already stated in Sect. 5.2). Therefore, Eq. 5.23 should be considered as just another way of expressing Eq. 5.20.

It follows from Eq. 5.22 that the lead field will never be homogeneous in real situations, because the current field through a volume conductor is in general never

homogeneous: it changes direction, and is weaker further away from the current source, as the same current passes through a larger surface. Furthermore, since $\sigma$ is also a function of position and is in general different for different volume conductors, it follows that the lead field $\frac{-\vec{J}_0^L}{\sigma}$ is different for different lead measurement locations, and different shapes and conduction characteristics of the volume conductor. This is the justification for the important assertions we made in Sect. 5.3 about the lead vector: it depends on the location of the dipole, on the locations of the lead electrodes, and on the electrical characteristics and the shape of the volume conductor, but not on the magnitude or the direction of the dipole.

A special and unrealistic case is a homogeneous volume source and a constant lead field $\vec{J}_0^{\,L} = \vec{J}_C$, which weights all elementary dipoles $\vec{J}^i dV$ equally. If we rewrite Eq. 5.20 by substituting $\frac{\nabla\phi_0''}{I_0}$ with $\frac{-\vec{J}_C}{\sigma I_0}$, we get:

$$L = \frac{-1}{I_0\sigma}\vec{J}_C \cdot \vec{p}_H. \tag{5.25}$$

By comparing Eq. 5.25 with the extended Burger's equation 5.11 we see that the measured lead voltage is obtained as a scalar product of the heart vector and the lead vector $\frac{-1}{I_0\sigma}\vec{J}_C$, which is independent of the location of $\vec{p}_H$. Consequently, if we were able to design a constant and known lead field, and under assumption of the volume source being homogeneous, we could obtain the heart vector $\vec{p}_H$ by using the procedure described in Sect. 5.3.3. In general, however, it is not practically possible to design a completely homogeneous lead field, because of the nature of the current distribution through a volume conductor, and because of the intrinsic inhomogeneity of real volume conductors.

An alternative, practical and applicable way of determining the heart dipole is the application of the Gabor-Nelson theorem, which, still under assumption of a homogeneous conductor, relates the heart dipole to the measurements of volume conductor surface potentials:

$$\vec{p}_H = \sigma \int_S \phi d\vec{S}, \tag{5.26}$$

where $\phi$ is the potential at the surface element $d\vec{S}$ and $\sigma$ is the conductivity of the body surface $S$. The Gabor-Nelson theorem has been used to practically estimate the heart vector [18], but it can also be used to find the location of the heart vector [19].

Like image surfaces, the lead fields are also computed by using models of a volume conductor. Some examples of computed lead fields are found in [20], where a computer thorax model developed from CT-scans has been used. Another more recent model is from Horáček et al., who used a boundary-element model of a realistic three-dimensional human torso containing lungs and intracavity blood masses of different conductivities, to calculate lead vectors of 1239 heart vector locations, for 352 unipolar body-surface leads [17].

## 5.6 Lead System Design—Differential Lead Positioning

An additional consequence of the reciprocity theorem is that if we wanted to catch each source element $\vec{J}^i dV$ with the same weight, i.e., with the same sensitivity, we would need a homogeneous, i.e., constant lead field $\nabla\phi_0''$. This fact is the main design guideline behind all the vectorcardiography (VCG) lead systems. On the other hand, a lead system may be targeted to a specific part and/or side of the heart. This is accomplished by designing leads that have lead fields stronger (larger $|\nabla\phi_0''|$) in a particular segment of the heart.

Let us first consider the lead field for a point electrode. The potential field and its gradient for a monopole [13] are given by:

$$\phi_M = \frac{I_M}{4\pi\sigma}\frac{1}{r}, \quad \nabla\phi_M = -\frac{I_M}{4\pi\sigma}\frac{1}{r^2}\vec{a}_r, \tag{5.27}$$

where $I_M$ is the monopole's source current strength, $\vec{r}$ is the radius vector for a point in space at which the field is evaluated, and $\vec{a}_r$ is the unit vector in the direction of $\vec{r}$. Since, according to Eq. 5.21, the lead field is equal to the gradient of the potential field caused by reciprocal current, $\nabla\phi_M$ is the lead field for a point electrode. From Eq. 5.27, it follows that $\nabla\phi_M$ decreases in magnitude with the square of the distance from the electrode. Consequently, this field will weight sources close to the electrode more heavily, by a square of the distance.

For a closely spaced electrode pair, also termed differential lead (DL), according to Eq. 5.21, the field will be the gradient of a dipole field. The potential field of a dipole $\vec{p}$ and its gradient [21] are given by:

$$\phi_D = \frac{\vec{a}_r \cdot \vec{p}}{4\pi\sigma}\frac{1}{r^2}, \quad \nabla\phi_D = -\frac{1}{4\pi\sigma}\frac{1}{r^3}[3(\vec{a}_r \cdot \vec{p})\vec{a}_r - \vec{p}], \tag{5.28}$$

which shows that a DL field weakens with the cube of the distance. Consequently, the source elements closer to the DL's electrodes' positions are weighted more strongly, by a factor of $r^3$. Therefore, DLs can be considered as very focused cardiac electrical activity detection devices. Moreover, DLs can be strategically placed so that their lead field obtains a particular property. Figure 5.4 illustrates the lead field of a DL.

It has been experimentally shown that DLs provide high quality ECG signals [22]. Most of the studies evaluating patch ECG monitors concentrate on arrhythmia detection. Studies done with a Philips experimental device featuring three DLs claim that the system provides high agreement with the EASI Holter monitor, in term of "evaluation of atrial activity, ventricular morphology, rhythm diagnosis" [23], as well as for "recognition of ventricular ectopic activity and ventricular fibrillation" [24]. An evaluation of Zio Patch [25] shows that the patch monitor detects more arrhythmic events than a conventional Holter monitor over the total wear time, but during 24-h it detected significantly less arrhythmic events than the Holter monitor. Clinical evaluation of the WPR Medical monitor shows better performance than the Holter monitor, but the authors conclude "that recorded ECG signals obtained

from the wireless ECG system had an acceptable quality for arrhythmia diagnosis" [26]. An evaluation of the Imec's ECG patch shows, on ten subjects, that "the new ECG patch has the same performance as a medical gold standard Holter" for atrial fibrillation detection [27]. Also, an evaluation of the ePatch [28] shows that it can be useful for rhythm analysis.

Investigations of the applicability of DLs for specific purposes other than arrhythmia detection have been scarce so far. Investigations in [29] and [30] show that a DL can provide better sensitivity for detecting left ventricular hypertrophy than the Sokolow-Lyon criterion on the 12-lead ECG. Furthermore, the so-called CM5 lead—the lead between the manubrium and the V5 position—is commonly used as an additional lead to the 12-lead ECG during an exercise electrocardiographic test. A recent report shows that CM5 contributes to increased sensitivity of the exercise ECG to the coronary artery disease [31].

## 5.7 ECG Leads Synthesis from Three Measured Leads—General Considerations

Synthesis of leads is a process of transforming one lead system into another. Measurements are available for the lead system being transformed, whereas the leads for the newly produced system are not measured (or at least some of the leads are not measured directly). Even though such transformation can be obtained in various ways, and can even be nonlinear, it is worth to consider it first as a linear transformation of lead vectors. For obtaining a fixed, i.e. time independent, linear transformation between two lead systems, we will assume that the heart is a fixed-location dipole, the body is a linear system with time-invariant conductivity, and there is no noise in measurements.

Assume two lead systems $\mathbb{S}_1 = \{S_1^1, \ldots, S_1^{m_1}\}$ and $\mathbb{S}_2 = \{S_2^1, \ldots, S_2^{m_2}\}$ with $m_1$ and $m_2$ leads. Under the aforementioned assumptions, we may employ the Burger's equation for every lead in both systems and for an arbitrary point in time:

$$\boldsymbol{S_1} = \vec{\boldsymbol{S}}_{\boldsymbol{1}} \cdot \vec{p}, \qquad \boldsymbol{S_2} = \vec{\boldsymbol{S}}_{\boldsymbol{2}} \cdot \vec{p}, \tag{5.29}$$

where $\boldsymbol{S_1}$ and $\boldsymbol{S_2}$ are one-column matrices of lead values, $\vec{\boldsymbol{S}}_{\boldsymbol{1}}$ and $\vec{\boldsymbol{S}}_{\boldsymbol{2}}$ are the matrices with $\mathbb{S}_1$ and $\mathbb{S}_2$ systems' lead vectors in rows, and $\vec{p}$ is a fixed-location dipole describing the heart (column vector). The matrices $\vec{\boldsymbol{S}}_{\boldsymbol{1}}$ and $\vec{\boldsymbol{S}}_{\boldsymbol{2}}$ have dimensions $m_1 \times 3$ and $m_2 \times 3$, respectively. Since three independent leads are necessary for describing a fixed-location dipole (Sect. 5.3.3), we will assume that the rank of $\vec{\boldsymbol{S}}_{\boldsymbol{1}}$ and $\vec{\boldsymbol{S}}_{\boldsymbol{2}}$ is 3.

We are searching for a linear transformation $\boldsymbol{X}$ that transforms $\boldsymbol{S_1}$ to $\boldsymbol{S_2}$:

$$\boldsymbol{S_2} = \boldsymbol{X} \cdot \boldsymbol{S_1}. \tag{5.30}$$

By combining Eqs. 5.29 and 5.30, we obtain $\vec{\boldsymbol{S}}_{\mathbf{2}} \cdot \vec{p} = \boldsymbol{X} \cdot \vec{\boldsymbol{S}}_{\mathbf{1}} \cdot \vec{p}$, which is true only if $\vec{\boldsymbol{S}}_{\mathbf{2}} = \boldsymbol{X} \cdot \vec{\boldsymbol{S}}_{\mathbf{1}}$.

Under the above assumptions, just three independent leads are sufficient for uniquely obtaining the dipole $\vec{p}$. Therefore, only three independent leads from $\vec{\boldsymbol{S}}_{\mathbf{1}}$ are sufficient to obtain the transformation $\boldsymbol{X}$. We will denote the matrix with three arbitrary, linearly independent leads from $\vec{\boldsymbol{S}}_{\mathbf{1}}$ as $\vec{\boldsymbol{S}}_{\mathbf{1}}{}^{*}$, so that we can write:

$$\vec{\boldsymbol{S}}_{\mathbf{2}} = \boldsymbol{X} \cdot \vec{\boldsymbol{S}}_{\mathbf{1}}{}^{*}, \tag{5.31}$$

where $\vec{\boldsymbol{S}}_{\mathbf{1}}{}^{*}$ is a square $3 \times 3$ matrix with the full rank and, hence, the inverse matrix $(\vec{\boldsymbol{S}}_{\mathbf{1}}{}^{*})^{-1}$ always exists. By multiplying Eq. 5.31 by $\vec{\boldsymbol{S}}_{\mathbf{1}}{}^{*^{-1}}$ from the right, we obtain:

$$\boldsymbol{X} = \vec{\boldsymbol{S}}_{\mathbf{2}} \cdot (\vec{\boldsymbol{S}}_{\mathbf{1}}{}^{*})^{-1}. \tag{5.32}$$

The equation tells how the linear transformation $\boldsymbol{X}$ between the lead systems $\mathbb{S}_1$ and $\mathbb{S}_2$ can be calculated directly from the lead vectors of both systems.

According to the discussion in Sect. 5.3.2, the lead vectors are obtained from a model of a human torso. By using such "generic" lead vectors for obtaining the transformation $\boldsymbol{X}$, one is ignoring the individual characteristics of the volume conductor and the $\vec{p}_H$ locations, on which the lead vectors depend. For this reason, and since the assumptions we have made are in reality not completely satisfied, the transformed lead values $\boldsymbol{X} \cdot \boldsymbol{S}_{\mathbf{1}}$ will in general deviate from the measured values, which can be expressed as:

$$\boldsymbol{S}_{\mathbf{2}} = \boldsymbol{X} \cdot \boldsymbol{S}_{\mathbf{1}} + \vec{\varepsilon}, \tag{5.33}$$

where $\vec{\varepsilon}$ is a column vector of differences between the synthesized and the measured values for each lead.

The transformation $\boldsymbol{X}$ depends only on the lead vectors of the two lead systems. These lead vectors, and consequently the transformation $\boldsymbol{X}$, are time-independent thanks to the assumption of a fixed heart vector and a constant conductivity. Still, if we are transforming between lead systems that have approximately homogeneous lead fields, i.e., similar lead vectors for different locations of the dipole, we can apply the transformation $\boldsymbol{X}$ without accepting that the heart dipole has a fixed location, i.e., by letting the dipole location to vary in time. This can be done because lead vectors in an approximately homogeneous lead field are similar in different locations.

If measurements from both lead systems $\mathbb{S}_1$ and $\mathbb{S}_2$ are a priori available for a person, it is obvious, from Eq. 5.33, that a personalized transformation $\boldsymbol{X}$ can be obtained with regression methods, even though there is no practical way of obtaining personalized lead vectors, as that would require a volume source and a volume conductor model to be constructed for each person. For that reason, researchers usually rely on regression to find a transformation between lead systems (more details in Sect. 5.8).

Regardless of the synthesis method, it is preferred that each lead picks up rich "information" about the cardiac electrical activity, preferably with complementary

"information" from those parts of the heart where the other leads are weaker. By considering Eq. 5.24, this is accomplished with leads having lead fields strong in their particular parts of the heart, since it is not practically possible to construct lead fields of a constant strength. This also ensures an adequate signal-to-noise ratio for at least one lead at a certain instant of time.

An additional consideration is the orthogonality of the lead vectors. According to the Burger's equation, as the angle between $\vec{p}$ and $\vec{L}$ approaches 90°, the measured voltage drops, which can cause a low signal-to-noise ratio for that lead. Therefore, we prefer orthogonal lead vectors, so that when $\vec{p}$ is nearly orthogonal to a certain lead, it has a large projection on at least one other lead vector.

### *5.7.1 Correctness of the Dipole Volume Source Model*

The linear transformation $\boldsymbol{X}$ between two lead systems, derived in the previous section, relies on the dipole model and, hence, neglects all the information about the cardiac electrical activity not explained by the dipole. Consequently, $\boldsymbol{X}$ is only as good as the dipole is a correct approximation for an equivalent source.

The output of the VCG lead systems is the path of the heart's dipole tip during the heart cycle. Consequently, any evaluation of the diagnostic content of a VCG system is also an evaluation of the dipole volume source model. Even though VCG is almost extinct from today's electrocardiography, there are studies providing evidence that it contains practically the same diagnostic information as the standard 12-lead ECG [32].

The Becking-Burger technique [33] is a way of measuring the non-dipole components of cardiac electrical activity by evaluating the quality of a lead, preferably close to the heart, synthesized from three independent leads, preferably at some distance from the heart. Even though the Becking-Burger technique usually uses orthogonal lead systems, it is also possible to use an arbitrary set of three linearly independent reference leads. Any evaluation of the leads synthesized from a system of three linearly independent leads can be considered as applying the Becking-Burger technique to multiple leads, i.e. the leads of the synthesized system. One of the most comprehensive evaluations of a derived ECG system, namely the EASI lead system, was conducted by Horàček et al. [17, 34] on a population of 892 individuals, mostly patients with a previous myocardial infarction. The results of this study also support the correctness of the dipole hypothesis.

## 5.8 Overview of Methods for the Synthesis of the 12-Lead ECG

Both linear and nonlinear methods have been used to model relations between ECG leads for the purpose of lead synthesis [35, 36]. The linear regression has been the most often utilized method [35]. Among the nonlinear methods, artificial neural networks (NNs) have been mostly used [37].

Recent publications, besides traditional methods, like multiple linear regression [38], report also some novel approaches for ECG leads synthesis, like support vector regression [39], regression trees [40], and state-space models [41]. Some researchers apply linear transformation on independent [42] or principal components [43–45], or on derived characteristics in the wavelet domain [46], instead of transforming original signals. Even though the derived characteristics in general do not contain all the information from the original signal, such transformations can be justified by the fact that the independent and principal component analysis can be efficient noise-filtering methods.

The deterministic method described in Sect. 5.7 was also sometimes used. This method takes lead vectors from an image surface and calculates the transformation matrix according to Eq. 5.32. Cao et al. used the deterministic approach to synthesize the 12-lead ECG from three DLs [47]. Rarely used is also the search method. Its concept is to form different transformation matrices $\boldsymbol{X}$ by incrementing elements in $\boldsymbol{X}$ by a predefined value. Among all the transformations $\boldsymbol{X}$ obtained in this way, the best $\boldsymbol{X}$ is the one that synthesizes the 12-lead ECG that is, in terms of the employed metrics, most similar to the target ECG. The metrics for comparing ECGs are presented in the next section.

## 5.9 Synthesis Evaluation

The quality of the synthesized 12-lead ECG is evaluated by comparing it to the target 12-lead ECGs obtained in the standard way. The most commonly used metrics for automatic evaluation are the root-mean-square distance (RMSD) and the correlation coefficient (CC). In parallel with these methods, it is often useful to engage an expert, i.e. a cardiologist, to examine independently the target and the synthesized ECGs. The synthesis is considered to be successful if both ECGs lead the cardiologist to the same conclusions.

## 5.10 Synthesis Personalization

The synthesis of the 12-lead ECG can be universal or adjusted to each person. Although, in general, both the transformation parameters and the electrode positions can be personalized, almost all existing derived 12-lead ECG systems employ universal electrode positions. An exception are the patch ECG body sensors that can be placed in an arbitrary position on the body surface, meaning that their positions can be personalized [48]. The transformations, on the other hand, are universal or personalized. The transformation matrix is generally calculated from the lead vectors (see Sect. 5.7). Any personalization of the transformation matrix can, therefore, be considered as an employment of personalized lead vectors.

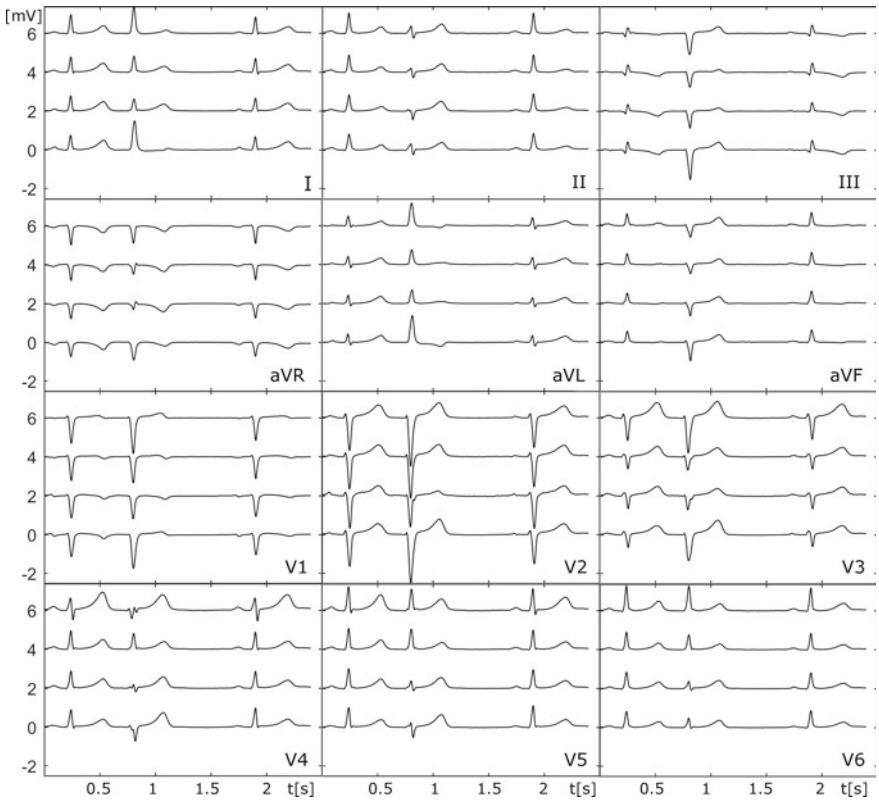


**Fig. 5.5** Target 12-lead ECG (the bottom curve in each panel) and three synthesized 12-lead ECGs (the curves moved up by 2, 4 and 6 mV) drawn in this bottom-up order: (*I*) personalized DL positions and personalized transformation, (*II*) universal DL positions and personalized transformation, (*III*) universal DL positions and universal transformation. The second beat is an extrasystole

Since it is not practically possible to obtain personalized lead vectors (Sect. 5.7), the personalized synthesis requires simultaneous measurement of the 12-lead ECG and the leads used for the synthesis, which have to be obtained for each person before the transformation can be calculated with, e.g., linear regression or NNs. The universal synthesis, on the other hand, can be obtained by using an image space, or with NNs or linear regression, whose inputs are obtained by juxtaposing measurements from different individuals [35].

There are two additional methods for the universal synthesis. One forms the universal transformation coefficients as the mean of the transformation coefficients obtained for each person. The other method is a modification of the search method: instead of assuming the best combination of parameters to be the one that produces the best synthesized ECG for a particular person, the selected transformation coefficients are those that result in the best synthesis, on average, over all considered measurements.

The advantage of a universal synthesis is that, once calculated, the transformation parameters can be applied to every person without a need for new measurements. The disadvantage is that a universal synthesis generally gives results that are inferior to those obtained by a personalized approach, because the universal transformation parameters are not adjusted to the anatomical uniqueness of each person.

As for the synthesis from DLs, there have been a few investigations showing that a reliable 12-lead ECG can be synthesized from them, with the personalized approach providing the best results [47–50]. Figure 5.5 shows a 12-lead ECG obtained from a cardiac patient (the bottom curve in each panel). The synthesized 12-lead ECGs are presented with the upper three curves. They have been obtained from three DLs, but with different approaches (in the bottom-up order): (I) personalized DL positions and personalized transformation, (II) universal DL positions and personalized transformation, and (III) universal positions and universal transformation. All ECG curves are visually alike, but a detailed analysis confirms that the first approach provides an ECG most similar to the target ECG.

The second beat of the target ECG from Fig. 5.5 is an extrasystole, which is synthesized appropriately in most of the leads, except in the leads II, aVR, aVL and V5. Extrasystoles are harder to synthesize because they can have a different electrical origin than the normal beats, which implies different heart vector positions. For this reason, extrasystoles can be considered as a rigorous input to a synthesis evaluation. Both DL positions and transformations could be tailored to extrasistolic events, and this is an interesting future research topic.

The universal DL positions used in the synthesis of the two upper ECG curves from Fig. 5.5 are shown in Fig. 5.6, marked by A, B, and C. They were found by using an algorithm published in [49]. The same algorithm was used to obtain the best personalized DL positions. The algorithm uses all the unipolar leads defined by the electrodes marked in Fig. 5.6 with black circles, to find three DLs that provide

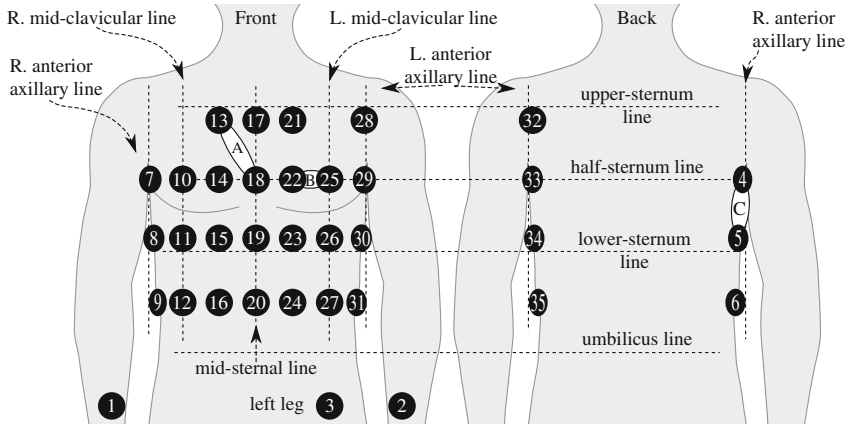


**Fig. 5.6** 35-channel ECG electrode positioning. The leads marked by *A*, *B*, and *C* are calculated as the best DLs for the 12-lead ECG synthesis

the best synthesis results. To find the universal DL positions marked in Fig. 5.6, the algorithm accepts juxtaposed ECG measurements from a number of patients and healthy persons, whereas for the personalized synthesis, the algorithm is fed with measurements from a single person. The best combination of three DLs provided by the algorithm is the one that produces synthesized 12-lead ECG with the biggest CC (see Sect. 5.9) to the target 12-lead ECG. For the synthesis from each triplet of DLs, linear regression was used.

## References


1. Rush, S., Abildskov, J.A., McFee, R.: Resistivity of body tissues at low frequencies. Circ. Res. **12**, 40–50 (1963)
2. Schwan, H.P., Kay, C.F.: The conductivity of living tissues. Ann. N. Y. Acad. Sci. **65**(6), 1007–1013 (1957)
3. Plonsey, R., Heppner, D.B.: Considerations of quasi-stationarity in electrophysiological systems. Bull. Math. Biophy. **29**(4), 657–664 (1967)
4. Frank, E.: Spread of current in volume conductors of finite extent. Ann. N. Y. Acad. Sci. **65**(6), 980–1002 (1957)
5. Malmivuo, J., Plosney, R.: Forward and inverse problem. In: Bioelectromagnetism. Oxford University Press (1995) (Chap. 7.5)
6. Geselowitz, D.: On bioelectric potentials in an inhomogeneous volume conductor. Biophys. J. **7**(1), 1–11 (1967)
7. Geselowitz, D.B.: Dipole theory in electrocardiography. Am. J. Cardiol. **14**(3), 301–306 (1964)
8. Einthoven, W.: The different forms of the human electrocardiogram and their signification. Lancet **179**(4622), 853–861 (1912) (originally published as Volume 1, Issue 4622)
9. Einthoven, W., Fahr, G., Waart, A.: Über die richtung und die manifeste grösse der potentialschwankungen im menschlichen herzen und über den einfluss der herzlage auf die form des elektrokardiogramms. Pflüger's Archiv für die gesamte Physiologie des Menschen und der Tiere **150**(6), 275–315 (1913)
10. Burger, H.C., Milaan, J.B.V.: Heart-vector and leads. Br. Heart J. **8**(3), 157–161 (1946)
11. Burger, H.C., Milaan, J.B.V.: Heart-vector and leads. Part ii. Br. Heart J. **9**(3), 154–160 (1947)
12. Malmivuo, J., Plosney, R.: Dipole. In: Bioelectromagnetism. Oxford University Press (1995) (Chap. 8.2)
13. Plonsey, R., Barr, R.C.: Sources and fields. In: Bioelectricity, pp. 23–43, 3rd edn. Springer, US (2007) (Chap. 2)
14. Frank, E.: General theory of heart-vector projection. Circ. Res. **2**(3), 258–270 (1954)
15. Burger, H.C., Milaan, J.B.V.: Heart-vector and leads. Part III (Geometrical Representation). Br. Heart J. **10**(4), 229–233 (1948)
16. Frank, E.: The image surface of a homogeneous torso. Am. Heart J. **47**(5), 757–768 (1954)
17. Horácek, B.M., Warren, J.W., Feild, D.Q., Feldman, C.L.: Statistical and deterministic approaches to designing transformations of electrocardiographic leads. J. Electrocardiol. **35**(4, Part B), 41–52 (2002)
18. Voukydis, P.C.: Application of the gabor-nelson theory in electrocardiography. Med. Biol. Eng. **10**(2), 223–229 (1972)
19. Malmivuo, J., Plosney, R.: Theoretical methods for analyzing volume sources and volume conductors. In: Bioelectromagnetism. Oxford University Press (1995) (Chap. 11)
20. Hyttinen, J.A.K., Malmivuo, J.A., Walker, S.J.: Lead field of ECG leads calculated by a computer thorax model-an application of reciprocity. In: Proceedings of Computers in Cardiology, pp. 241–244 (1993)

21. Griffiths, D.J.: The electric field of a dipole. In: Introduction to Electrodynamics, pp. 153–155, 3rd edn. Prentice Hall (1999) (Chap. 3.4.4)
22. Puurtinen, M., Viik, J., Hyttinen, J.: Best electrode locations for a small bipolar ECG device: signal strength analysis of clinical data. Ann. Biomed. Eng. **37**(2), 331–336 (2009)
23. Janata, A., Lemmert, M.E., Russell, J.K., Gehman, S., Fleischhackl, R., Robak, O., Pernicka, E., Sterz, F., Gorgels, A.P.: Quality of ECG monitoring with a miniature ECG recorder. Pacing Clin. Electrophysiol. **31**(6), 676–684 (2008)
24. Lemmert, M.E., Janata, A., Erkens, P., Russell, J.K., Gehman, S., Nammi, K., Crijns, H.J., Sterz, F., Gorgels, A.P.: Detection of ventricular ectopy by a novel miniature electrocardiogram recorder. J. Electrocardiol. **44**(2), 222–228 (2011)
25. Barrett, P.M., Komatireddy, R., Haaser, S., Topol, S., Sheard, J., Encinas, J., Fought, A.J., Topol, E.J.: Comparison of 24-hour Holter monitoring with 14-day Novel adhesive patch electrocardiographic monitoring. Am. J. Med. **127**(1), 95.e11–95.e17 (2014)
26. Fensli, R., Gundersen, T., Snaprud, T., Hejlesen, O.: Clinical evaluation of a wireless ECG sensor system for arrhythmia diagnostic purposes. Med. Eng. Phys. **35**(6), 697–703 (2013)
27. Torfs, T., Smeets, C.J., Geng, D., Berset, T., der Auwera, J.V., Vandervoort, P., Grieten, L.: Clinical validation of a low-power and wearable ECG patch for long term full-disclosure monitoring. J. Electrocardiol. **47**(6), 881–889 (2014)
28. Saadi, D., Fauerskov, I., Osmanagic, A., Sheta, H., Sorensen, H., Egstrup, K., Hoppe, K.: Heart rhythm analysis using ECG recorded with a novel sternum based patch technology: a pilot study. In: Proceedings of the International Congress on Cardiovascular Technologies (CARDIOTECHNIX), pp. 15–21 (2013)
29. Väisänen, J., Puurtinen, M., Hyttinen, J., Viik, J.: Short Distance bipolar electrocardiographic leads in diagnosis of left ventricular hypertrophy. Comput. Cardiol. **37**, 293–296 (2010)
30. Puurtinen, M., Väisänen, J., Viik, J., Hyttinen, J.: New precordial bipolar electrocardiographic leads for detecting left ventricular hypertrophy. J. Electrocardiol. **43**(6), 654–659 (2010)
31. Puurtinen, M., Nieminen, T., Kähönen, M., Lehtimäki, T., Lehtinen, R., Nikus, K., Hyttinen, J., Viik, J.: Value of leads V4R and CM5 in the detection of coronary artery disease during exercise electrocardiographic test. Clin. Physiol. Funct. Imaging **30**(4), 308–312 (2010)
32. Willems, J.L., Lesaffre, E., Pardaens, J.: Comparison of the classification ability of the electrocardiogram and vectorcardiogram. Am. J. Cardiol. **59**(1), 119–124 (1987)
33. Burger, H.C.: Lead vector projections. I., Ann. N. Y. Acad. Sci. **65**(6), 1076–1087 (1957)
34. Horácek, B.M., Warren, J.W., Stóvícek, P., Feldman, C.L.: Diagnostic accuracy of derived versus standard 12-lead electrocardiograms. J. Electrocardiol. **33**(Supplement 1), 155–160 (2000)
35. Tomašić, I., Trobec, R.: Electrocardiographic systems with reduced numbers of leads – Synthesis of the 12-lead ECG. IEEE Rev. Biomed. Eng. **7**, 126–142 (2014)
36. Vozda, M., Cerny, M.: Methods for derivation of orthogonal leads from 12-lead electrocardiogram: a review. Biomed. Signal Process. Control **19**, 23–34 (2015)
37. Atoui, H., Fayn, J., Rubel, P.: A novel neural-network model for deriving standard 12-lead ECGs from serial three-lead ECGs: application to self-care. IEEE Trans. Inform. Technol. Biomed. **14**(3), 883–890 (2010)
38. Figueiredo, C.P., Mendes, P.M.: Towards wearable and continuous 12-lead electrocardiogram monitoring: Synthesis of the 12-lead electrocardiogram using 3 wireless single-lead sensors. In: Proceedings of the International Conference on Biomedical Electronics and Devices (BIODEVICES), pp. 329–332 (2012)
39. Yodjaiphet, A., Theera-Umpon, N., Auephanwiriyakul, S.: Electrocardiogram reconstruction using support vector regression. In: Proceedings of the IEEE International Symposium on Signal Processing and Information Technology (ISSPIT), pp. 000269–000273 (2012)
40. Tomasic, I., Trobec, R., Lindén, M.: Can the regression trees be used to model relation between ECG leads? In: Internet of Things. IoT Infrastructures: Second International Summit, pp. 467–472. Springer International Publishing (2016)
41. Lee, J., Kim, M., Kim, J.: Reconstruction of precordial lead electrocardiogram from limb leads using the state-space model. IEEE J. Biomed. Health Informat. **20**(3), 818–828 (2016)

42. Tsouri, G.R., Ostertag, M.H.: Patient-specific 12-lead ECG reconstruction from sparse electrodes using independent component analysis. IEEE J. Biomed. Health Informat. **18**(2), 476–482 (2014)
43. Tomašić, I., Skala, K., Trobec, R.: Principal component analysis and visualization in optimization and personalization of lead's set for generation of standard 12-leads ECG. In: Proceedings of the 31th International Convention on Information and Communication Technology, Electronics and Microelectronics, pp. 307–313 (2008)
44. Mann, S., Orglmeister, R.: PCA-based ECG lead reconstruction. Biomedizinische Technik. Biomed. Eng. **58**(Supp. 1), 24–25 (2013)
45. Dawson, D., Yang, H., Malshe, M., Bukkapatnam, S.T.S., Benjamin, B., Komanduri, R.: Linear affine transformations between 3-lead (Frank XYZ leads) vectorcardiogram and 12-lead electrocardiogram signals. J. Electrocardiol. **42**(6), 622–630 (2009)
46. Nallikuzhy, J.J., Dandapat, S.: Enhancement of the spatial resolution of ECG using multiscale Linear Regression. In: Proceedings of the 21st National Conference on Communications (NCC), pp. 1–6 (2015)
47. Cao, H., Li, H., Stocco, L., Leung, V.C.M.: Wireless three-pad ECG system: challenges, design, and evaluations. J. Commun. Netw. **13**(2), 113–124 (2011)
48. Trobec, R., Tomašić, I.: Synthesis of the 12-lead electrocardiogram from differential leads. IEEE Trans. Inf. Technol. Biomed. **15**(4), 615–621 (2011)
49. Tomašić, I., Frljak, S., Trobec, R.: Estimating the universal positions of wireless body electrodes for measuring cardiac electrical activity. IEEE Trans. Inf. Technol. Biomed. **60**(12), 3368–3374 (2013)
50. Hansen, I.H., Hoppe, K., Gjerde, A., Kanters, J.K., Sorensen, H.B.D.: Comparing twelve-lead electrocardiography with close-to-heart patch based electrocardiography. In: Proceedings of the 37th Annual International Conference of the IEEE Engineering in Medicine and Biology Society (EMBC), pp. 330–333 (2015)